AMERICAN ACADEMY OF OPHTHALMOLOGY®

Reticular Pseudodrusen

Impact of Their Presence and Extent on Local Rod Function in Age-Related Macular Degeneration

Himeesh Kumar, MBBS(Hons), PhD,[1,2] *Robyn H. Guymer, MBBS, PhD,*[1,2] *Lauren A.B. Hodgson, MPH,*[1] *Xavier Hadoux, MEng, PhD,*[1,2] *Maxime Jannaud, MEng,*[1] *Peter van Wijngaarden, MBBS(Hons), PhD,*[1,2] *Chi D. Luu, PhD,*[1,2,*] *Zhichao Wu, BAppSc(Optom), PhD*[1,2,*]

Purpose: To understand the spatial relationship between local rod-mediated visual function and reticular pseudodrusen (RPD) in eyes with large drusen.

Design: Retrospective cross-sectional study.

Participants: One eye with large drusen (>125 μm) each from 91 individuals with intermediate age-related macular degeneration, with and without RPD.

Methods: All participants underwent dark adaptation testing using a dark-adapted chromatic perimeter, where visual sensitivities were measured over 30 minutes of dark adaptation after photobleach. The rod intercept time (RIT; a measure of dynamic rod function) and pointwise sensitivity difference (PWSD; a relative measure of rod- compared with cone-mediated function) was determined at multiple retinal locations, and their association with the overall (central 20° × 20° region) and local (2° diameter region centered on the location tested) extent of RPD and drusen (quantified using multimodal imaging) was examined.

Main Outcome Measures: Association between overall and local extent of RPD and drusen with RIT and PWSD at each retinal location tested.

Results: In a multivariable analysis, delayed RIT was associated with an increasing overall ($P < 0.001$), but not local ($P = 0.884$), extent of RPD. In contrast, the increasing local ($P < 0.001$), but not overall ($P = 0.475$), extent of drusen was associated with delayed RIT. Furthermore, only an increasing overall extent of RPD ($P < 0.001$) was associated with reduced PWSD (or worse rod compared with cone function), but not the local extent of RPD and drusen, or overall extent of drusen ($P \geq 0.344$).

Conclusions: Local rod-mediated function was associated with the overall, rather than local, extent of RPD in eyes with large drusen, suggesting that there may be widespread pathologic changes in eyes with RPD that account for this.

Financial Disclosure(s): Proprietary or commercial disclosure may be found in the Footnotes and Disclosures at the end of this article. *Ophthalmology Science 2024;4:100551*

Reticular pseudodrusen (RPD), or subretinal drusenoid deposits, are seen on OCT imaging as distinctive subretinal accumulations located above the retinal pigment epithelium and are increasingly recognized as an important phenotype of age-related macular degeneration (AMD).[1] Studies have reported RPD as a risk factor for late AMD development[2–5] and faster rate of geographic atrophy lesion growth.[6,7] Indeed, the presence of RPD in eyes with large drusen was also a significant treatment effect modifier in a post hoc analysis of a randomized controlled trial of a novel subthreshold nanosecond laser to slow intermediate AMD progression.[8] In that study, a beneficial treatment effect was observed in eyes without RPD, whereas eyes with RPD showed worse treatment outcomes.[8] Histologic and clinical studies have also indicated that photoreceptors[9–12] and the retinal pigment epithelium[9] seem more abnormal in regions with RPD than those without.

With respect to the pathophysiology of RPD, numerous studies have reported that the presence of RPD is associated with impaired dark adaptation (i.e., delayed recovery of visual sensitivity under scotopic conditions after a photobleach)[13–18] and dark-adapted visual sensitivities (under scotopic conditions, after a specific period of dark adaptation, without photobleach)[18,19] when compared with similarly staged AMD eyes without RPD. Such impairments in dark adaptation and dark-adapted visual sensitivities have been reported to be present above and beyond the impairments that are already seen in eyes with large drusen and without RPD.[13,14,16] However, it remains to be clearly established whether impaired dark adaptation

https://doi.org/10.1016/j.xops.2024.100551
ISSN 2666-9145/24

is spatially correlated with the distribution of the RPD lesions, or if such impairments occur more broadly within the retina of eyes with RPD. Our recent study suggested that although regions with RPD demonstrated impaired mesopic visual sensitivity (primarily reflecting cone-mediated visual function[20–22]), these impairments were more strongly associated with the total extent of RPD than their extent in the region tested.[23]

These findings indicate that there may be widespread pathogenic changes in eyes with RPD. This study thus aimed to characterize the spatial relationship between rod-mediated visual dysfunction and RPD in eyes with large drusen.

Methods

This is a retrospective, cross-sectional study that included 1 eye with large drusen from each participant with intermediate AMD enrolled in observational studies of AMD at the Centre for Eye Research Australia (CERA). These studies were approved by the local institutional review board and were conducted according to the International Conference on Harmonization Guidelines for Good Clinical Practice and the tenets of the Declaration of Helsinki. All participants provided written informed consent before enrollment in these studies.

Participants and Procedures

This study included 1 eye from participants aged ≥50 years with ≥1 large drusen (>125 μm) and without any signs of late AMD defined on multimodal imaging. Late AMD was defined by the presence of the following: (1) exudative neovascular AMD (based on evidence of fluid on OCT imaging confirmed by changes seen on fluorescein and/or indocyanine green angiography as appropriate), (2) color fundus photography-defined geographic atrophy, or (3) OCT-defined nascent geographic atrophy[24] or more progressed forms of OCT atrophy. All included eyes had a best corrected visual acuity of 20/40 or better and had completed dark adaptation testing. Individuals who had undergone an experimental intervention for AMD (such as nanosecond laser) in either eye, or any other ocular disease that could compromise visual function or the assessment of the retina, were excluded from this study.

Assessment of Rod-Mediated Function

Rod-mediated function was evaluated using a dark-adapted chromatic perimeter (DACP; Medmont Pty Ltd), as described previously.[13,14] In brief, dark adaptation testing was performed monocularly after pupil dilation (requiring a minimum pupil size of 7 mm) and with correction of refractive error for a viewing distance of 30 cm. Testing was performed on the eye with worse visual acuity, with the fellow eye patched in a completely dark room using a Goldmann Size V stimulus (1.73° diameter). Fixation was monitored manually throughout testing with an infrared camera by the examiner, who encouraged the participant to maintain fixation when fixation drifts were observed.

Full-field flash bleaching of approximately 20% of the rod photopigments (with pupil size of 8-mm diameter)[25] was performed with a customized Ganzfeld light source[26] (~6.3 log Td sec) before visual sensitivity measurements. Testing commenced with cyan (505 nm) stimuli. Each perimetric test lasted approximately 1 minute. To examine rod function recovery, multiple perimetric tests (range 11–14 tests) were performed within 30 minutes of photobleaching, and participants were given time to rest between tests. A single perimetric examination with red (625 nm) stimuli was performed at the end of the cyan test.

Dark adaptation testing was performed using 1 of 3 stimulus patterns (as this was a retrospective study that included DACP testing data from different studies conducted at CERA) as shown in Figure 1. Grids A, B,[27] and C[13,28] consisted of 12, 16, and 14 test locations, respectively, with 8, 16, and 12 respective test locations falling within the central 20° × 20° region where the OCT volume scan was acquired. Only data for test locations that fell within this region were included in the analysis for this study because the pathologic features of interest (RPD and drusen extent) were only quantified in this region.

Rod-mediated visual function was assessed using rod intercept time (RIT).[14,29] At each test location, the RIT was calculated by fitting an exponential decay function (a dark adaptation curve) to visual sensitivity thresholds for the cyan stimuli to determine the recovery of rod sensitivity after photobleaching (Fig 2).[26] The RIT was defined as the time required for visual sensitivity to the cyan stimuli to reach a rod criterion level of −3 log units of stimulus intensity (Fig 2). For test points that did not reach the rod criterion level within 30 minutes, a RIT of 30 minutes was assigned. Rod-mediated function was also assessed using the 2-color perimetry technique.[14] The pointwise sensitivity difference (PWSD) between the thresholds for the last tests with the cyan and red stimuli was calculated to provide a relative measure of rod- compared with cone-mediated visual function, whereby a smaller PWSD indicates a larger degree of rod than cone impairment.[30]

Image Acquisition, Grading, and Analysis

All participants underwent multimodal imaging of the retina, including color fundus photography using the Canon CR6-45NM camera (Canon) and combined near-infrared reflectance (NIR) and OCT imaging using the Spectralis HRA+OCT device (Heidelberg Engineering). OCT volume scans covered a 20° × 20° region centered on the fovea and, depending on the study protocol (as this was a retrospective study), consisted of either 49 horizontal B-scans with 25 frames averaged per B-scan or 97 horizontal B-scans with 16 frames averaged per B-scan, all with 1024 A-scans per B-scan. A 30° × 30° NIR image of resolution 1536 × 1536 pixels was simultaneously captured with the OCT volume scan.

Color fundus photographs were graded for the presence of large drusen (>125 μm) and pigmentary abnormalities within 2-disc diameters of the fovea. Combined OCT and NIR images were graded for the presence of RPD, which was considered present if there were ≥5 definite lesions on ≥2 B-scans on OCT imaging that corresponded with definite lesions seen on NIR imaging. The grading of RPD was performed by 2 experienced graders (H.K. and L.A.B.H.), and any disagreements in grading were adjudicated by a senior medical retina specialist (R.H.G.). All 3 graders were masked to the results of the dark adaptation testing. The 2-dimensional area of RPD on NIR imaging was then annotated by an experienced grader (H.K.) using a custom software program (Cross-Modality Annotation Software [XMAS]; CERA)[31] by outlining the region(s) where the lesions were visible on both NIR and OCT imaging; an example of the annotations is shown in Figure 1 in which RPD extent is outlined. All annotations were then reviewed by a senior medical retina specialist (R.H.G.) with any disagreements resolved by open adjudication, and the annotations were revised based on consensus. OCT volume scans were used to calculate drusen volume using a convolutional neural network-based approach, as described previously.[32]

The local RPD area and drusen volume within a 2° diameter region centered on each retinal location used in dark adaptation

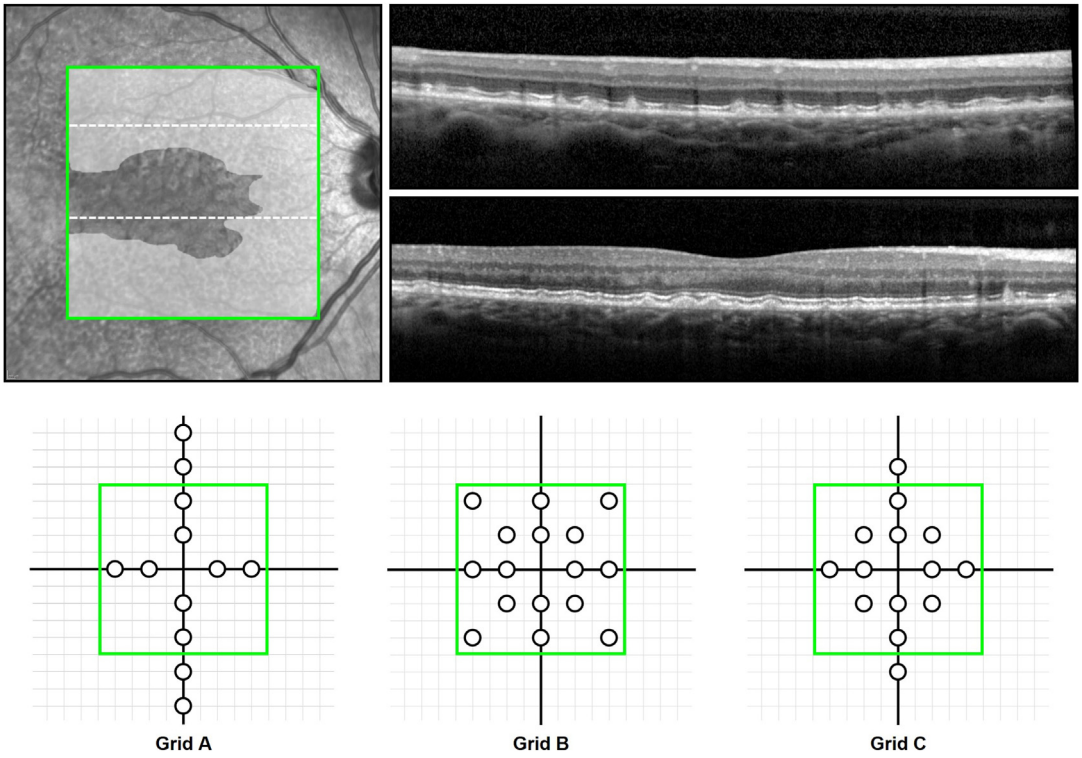

Figure 1. Annotation of reticular pseudodrusen (RPD) and stimulus patterns used for dark adaptation testing in this study. **A,** Example of how the extent of RPD was annotated (white overlay) within a 20° × 20° region where the OCT volume scan was acquired (green box), shown on the near-infrared reflectance (NIR), based on characteristic features seen on both modalities. Exemplary B-scans are shown in **B** and **C**; their locations correspond to the superior and inferior dashed lines respectively in **A**, with the former showing a B-scan where RPD was present throughout, and the latter showing RPD present only nasally (note also that some prominent drusen are also visible in the center of this B-scan). **D,** Three different stimulus patterns used for dark adaptation testing are shown, with the 20° × 20° region of the central macula shown (where OCT imaging was performed; green box), and only test locations within this region were included in the analyses of this study (as only these locations had corresponding RPD annotation data). Horizontal and vertical grid lines at 2° intervals are also shown.

testing were measured. In addition, overall RPD extent in the 20° × 20° OCT volume scan was calculated. Reticular pseudodrusen area and drusen volume measurements were square-root and cube-root transformed, respectively, to eliminate heteroskedasticity.

Statistical Analysis

The analyses in this study included all eyes with large drusen, with or without RPD, to examine the association between the presence, extent, and spatial correspondence of RPD and local RIT. A multivariable linear mixed model was first used to examine the association between the presence and local extent of RPD (i.e., the RPD area within the 2° diameter region centered on a DACP test location) and local drusen volume with RIT, adjusted for the potential confounders of age, pigmentary abnormalities, and eccentricity of the test location.[13,14,18] Correlations between test locations within an eye were adjusted by specific random intercepts at the eye level. A second multivariable linear mixed model including both the local and overall extent of RPD and drusen was used to examine whether the overall extent of either of these features were associated with RIT. This facilitated an analysis to understand if the local and/or global extent of each type of pathology was independently associated with RIT. Both analyses were repeated for PWSD, the other relative measure of rod- compared with cone-mediated visual function. Statistical analyses were performed using Stata software version 16.1 (StataCorp).

Results

A total of 91 eyes of 91 participants with an average age of 70 ± 8 years (range, 51−86 years) were included in this study. The median drusen volume in the 20° × 20° OCT volume scan region of the eyes included was 0.25 mm^3 (interquartile range = 0.09−0.44 mm^3). Reticular pseudodrusen and pigmentary abnormalities were present in 20 (22%) and 49 (54%) eyes, respectively. Among eyes with RPD, the median area of RPD in the 20° × 20° OCT scan region was 19.2 mm^2 (interquartile range = 8.6−24.4 mm^2). A total of 52 (57%), 22 (24%), and 17 (19%) eyes underwent dark adaptation testing with grids A, B, and C, respectively (Fig 1; consisting of 8, 16, and 12 stimuli that fell within the central 20° × 20° region), resulting in a total of 972 test locations analyzed in this study. Note that 37 (41%) of the eyes included in this study were part of studies that have been published previously.[13,27]

Association between RPD, Drusen, and Dark Adaptation Parameters

In the first multivariable model, the RIT at each tested location was significantly delayed (i.e., indicative of worse

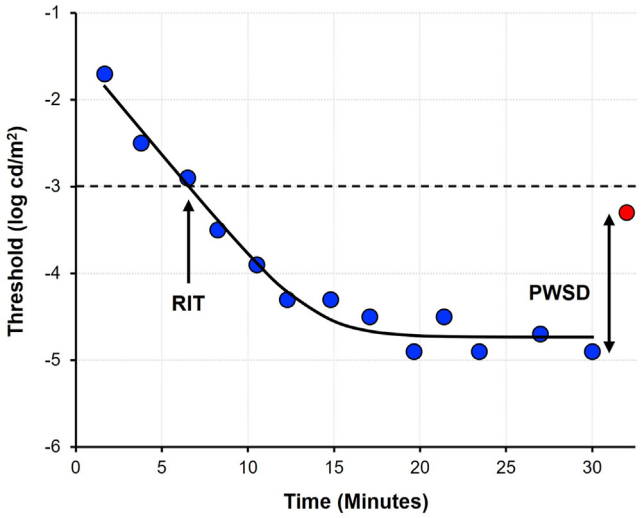

Figure 2. Example of a dark adaptation curve derived from visual sensitivity thresholds measured with cyan (505 nm) stimuli (indicated by blue filled markers), which were fitted with an exponential decay function (black line). The rod intercept time (RIT; time for visual sensitivity to the cyan stimuli to reach −3 log units of stimulus intensity) is indicated by the single-headed arrow, and the pointwise sensitivity difference (PWSD; difference in the last threshold estimates with the cyan [blue circular marker] and red [625 nm] stimuli) red circular marker is indicated by the double-headed arrow.

rod-mediated visual function) in eyes with RPD based on the overall presence of RPD and increasing drusen extent at the location tested ($P < 0.001$ for both) but not the local RPD extent ($P = 0.596$; Table 1).

In the second multivariable model, the overall extent of RPD and local extent of drusen were significantly associated with local RIT ($P < 0.001$), but the local extent of RPD and the overall extent of drusen were not ($P \geq 0.600$; Table 1).

For the outcome of PWSD, the first model showed that the overall presence of RPD ($P < 0.001$), but not the local extent of RPD or drusen ($P \geq 0.407$), was associated with a smaller sensitivity difference (indicative of a greater degree of rod- than cone-mediated visual function impairment; Table 2). The second model showed that the PWSD was significantly smaller with an increasing overall RPD extent ($P < 0.001$) but not the local extent of RPD or local or overall extent of drusen ($P \geq 0.373$; Table 2).

Discussion

In this study, we observed in eyes with large drusen from individuals with intermediate AMD that local reductions in rod-mediated visual function based on the RIT were associated with an increasing overall extent of RPD within the central 20° × 20° region, rather than the local extent of RPD. In contrast, our analysis showed that it was an increasing local, rather than overall, extent of drusen that was associated with worsening RIT. These findings suggest that the extent of RPD may be an indicator of diffuse pathologic changes in the macula.

Table 1. Association between Reticular Pseudodrusen (RPD), Drusen and Rod Intercept Time (RIT; Measured in mins) at Each Location Tested

	Coefficient (95% CI)	*P*-Value
Model 1:		
Overall RPD presence (yes)	9.6 (6.6 to 12.6)	<0.001
Local RPD extent (per mm*)	0.7 (-1.8 to 3.1)	0.596
Local drusen volume (per mm†)	0.9 (0.6 to 1.3)	<0.001
Model 2:		
Local RPD extent (per mm*)	0.2 (-2.3 to 2.6)	0.884
Overall RPD extent (per mm*)	2.5 (1.8 to 3.2)	<0.001
Local drusen volume (per mm†)	0.9 (0.6 to 1.3)	<0.001
Overall drusen volume (per mm†)	-0.2 (-0.7 to 0.3)	0.475

*Square root transformed.
†Cube root transformed; all models 1 and 2 were adjusted for age, presence of pigmentary abnormalities in the eye, and eccentricity of the test location.

In this study, we first performed a conventional analysis of whether the presence of RPD in the central 20° × 20° region and the increasing local extent of RPD and drusen were associated with delayed RIT. This analysis showed that the presence of RPD in eyes with large drusen is associated with worse dark adaptation than eyes with large drusen alone, consistent with previous studies that have reported greater delays in RIT for eyes with RPD than those without.[13–18] This analysis also showed that the local extent of drusen was independently associated with worsening RIT, which is consistent with the findings from Sevilla et al,[17] who similarly observed a significant association between the local retinal pigment epithelium–drusen complex volume and worsening local RIT. These findings are also consistent with the study by Laíns et al,[15] who reported a significant difference in RIT at a single test location based on the presence of drusen at that location tested. However, we did not find an independent association between the local extent of RPD and worsening RIT after accounting for the overall presence of RPD and local drusen volume.

We undertook a second analysis that included both the overall and local extent of RPD and drusen in the same multivariable model to understand their associations with RIT. This analysis uniquely demonstrated that local RIT was significantly associated with the overall, rather than local, extent of RPD. The opposite was observed for drusen, where the increasing local (but not overall) extent was associated with worse RIT. This spatially correspondent structure–function association was similarly observed by Laíns et al,[15] who reported a significant difference in RIT based on the presence of drusen at the single location tested but not on the overall presence of drusen in an eye. These findings are consistent with those of our recent study evaluating mesopic visual sensitivities using microperimetry (which primarily reflects cone-mediated visual function[20–22]), where it was observed that the overall, rather than the local, extent of RPD was most associated with function loss.[23]

Although RIT provides a direct measure of rod photoreceptor function, this study also evaluated PWSD, which

Table 2. Association between Reticular Pseudodrusen (RPD), Drusen and Pointwise Sensitivity Difference between the Cyan (505 nm) and Red (625 nm) Stimuli (Measured in Decibels [dB]) at Each Location Tested

	Coefficient (95% CI)	*P*-Value
Model 1:		
Overall RPD presence (yes)	-8.2 (-10.1 to -6.3)	<†0.001
Local RPD extent (per mm*)	-0.2 (-2.9 to 2.6)	0.914
Local drusen volume (per mm†)	0.2 (-0.3 to 0.6)	0.479
Model 2:		
Local RPD extent (per mm*)	1.4 (-1.5 to 4.2)	0.344
Overall RPD extent (per mm*)	-2.2 (-2.6 to -1.8)	<0.001
Local drusen volume (per mm†)	0.1 (-0.3 to 0.6)	0.548
Overall drusen volume (per mm†)	0.1 (-0.2 to 0.4)	0.453

*Square root transformed.
†Cube root transformed; all models 1 and 2 were adjusted for age, presence of pigmentary abnormalities in the eye, and eccentricity of the test location.

provides a relative measure of rod- compared with cone-mediated photoreceptor function based on the visual sensitivity difference to the cyan and red stimuli at a 30-minute criterion time. A reduction in sensitivity difference would indicate greater rod dysfunction than cone function (the latter of which could either be normal or abnormal). In contrast to the findings based on the RIT, we observed in the second analysis (that included both the overall and local extent of RPD and drusen) that only the increasing overall extent of RPD was significantly associated with reduced PWSD. Within the context of previous findings indicating that the presence of RPD is also associated with cone-mediated visual sensitivity deficits,[23,33–36] this suggests that an increasing overall extent of RPD—but not local drusen extent—appears to have a preferential impact on local rod-mediated visual sensitivity.

The findings in this study, and those of our previous study,[23] indicate that there may be diffuse pathogenic changes occurring in eyes with RPD. The notion of a generalized pathogenic change is supported by our previous histopathologic examination of an eye with RPD, where we observed widespread retinal stress as indicated by the upregulation of an intermediate filament for gliosis throughout the retina (glial fibrillary acidic protein).[9] Further research is needed to identify drivers of these diffuse pathogenic changes, which may provide further insights into the underlying pathogenesis of RPD. Such work could include further investigations into whether changes in other structural parameters seen on OCT imaging—such as those related to the photoreceptors[37–40] and choroid[15,16,41]—could account for these observations.

Strengths of this study include the topographic evaluation of dark adaptation using the DACP, a device with a sufficient dynamic range for this task,[30] enabling the evaluation of local structure–function associations. Other strengths include the relatively large size of the cohort evaluated, rigorous phenotyping of the participants included in this study, careful en face quantification of RPD using multimodal imaging that was verified by a senior retinal specialist, and the comprehensive adjustments for potential confounders of visual function.

Limitations of this study include the inclusion of only eyes with large drusen, and thus, the generalizability of these findings to earlier stages of AMD is unknown. Another limitation of this study is the use of a perimeter where fundus tracking was not available, meaning that variations in the retinal locations from fixation drifts during testing could not be accounted for and that the retinal locations sampled by the stimuli were estimated, rather than directly visualized. Nonetheless, we were still able to find a significant relationship between local RIT and local drusen volume, suggesting that the lack of fundus tracking did not prohibit the assessment of structure–function associations in this study. Such a local structure–function relationship was also observed in the study by Laíns et al[15] as described previously, using a device that also did not have fundus tracking. Note that there is currently no commercially available fundus-tracked perimeter with a sufficient dynamic range to topographically assess dark adaption.[13] In addition, during testing, the fixation was monitored manually and not with the Heijl–Krakau method typically used with standard automated perimetry, which is also not performed with another commercially available device for measuring dark adaptation at a single test location.[15–17] However, a recent study showed that fixation losses based on the Heijl–Krakau method had little impact on testing reliability,[42] and the absence of fixation monitoring with this strategy also did not prohibit the finding of a significant local structure–function relationship, as described here. A further limitation was the use of 3 different stimulus patterns in the evaluation of RIT and PWSD in study eyes, because this was a retrospective study that included all those who underwent DACP testing across different previous studies at our center. However, note that the findings of this study remain unchanged when evaluating only the 8 stimulus locations that were consistent across all 3 stimulus patterns (data not shown). Finally, the assessment and quantification of RPD was based on subjective grading, which we have recently shown does not exhibit near-perfect interreader agreement.[43] This study also only quantified the extent of RPD present in the central 20° × 20° region where the OCT volume scan was acquired, and it is possible that quantifying the extent of RPD present in a larger field of view (such as through using widefield OCT imaging) may result in different observations for the association between total RPD extent and local rod function. This requires further investigation in future studies.

In conclusion, this study demonstrated that local rod-mediated visual function is significantly associated with the overall, rather than the local, extent of RPD in eyes with large drusen from individuals with intermediate AMD. This is in contrast to the impact of drusen, where the converse was true. These findings suggest that there are likely to be diffuse pathogenic changes in eyes with RPD that account for variations in local rod-mediated visual sensitivity.

Footnotes and Disclosures

Originally received: March 8, 2024.
Final revision: April 29, 2024.
Accepted: April 30, 2024.
Available online: May 8, 2024. Manuscript no. XOPS-D-24-00078R1.

[1] Centre for Eye Research Australia, Royal Victorian Eye and Ear Hospital, East Melbourne, Australia.

[2] Department of Surgery (Ophthalmology), The University of Melbourne, Melbourne, Australia.

*C.D.L. and Z.W. contributed equally as senior authors.

Disclosure(s):

All authors have completed and submitted the ICMJE disclosures form.

The author(s) have made the following disclosure(s):

R.H.G: Personal fees − Apellis, Bayer, Novartis, Roche/Genentech outside the submitted work.

P.v.W.: Personal fees − Bayer Australia, Roche/Genentech outside the submitted work.

The other authors have no proprietary or commercial interest in any materials discussed in this article.

Supported by the National Health & Medical Research Council of Australia (project grant no.: GNT1181010 [RHG], GNT1194667 [RHG], #2008382 [ZW]), and grants from the Macular Disease Foundation Australia (RHG, CDL, and ZW), the BrightFocus Foundation (grant no.: M2019073 [ZW]), H&L Hecht Trust (XH, MJ, and PvW), and Centre for Eye Research Australia (CERA) Innovation Fund (XH, MJ, and PvW). CERA receives operational infrastructure support from the Victorian Government. The sponsor or funding organization had no role in the design or conduct of this research.

HUMAN SUBJECTS: Human subjects were included in this study. These studies were approved by the local institutional review board and were conducted according to the International Conference on Harmonization Guidelines for Good Clinical Practice and the tenets of the Declaration of Helsinki. All participants provided written informed consent before enrollment in these studies.

No animal subjects used included in this study.

Author Contributions:

Conception and design: Kumar, Guymer, Luu, Wu

Data collection: Kumar, Guymer, Hodgson, Luu, Wu

Analysis and interpretation: Kumar, Guymer, Hodgson, Hadoux, Jannaud, van Wijngaarden, Luu, Wu

Obtained funding: N/A

Overall responsibility: Kumar, Guymer, Hodgson, Hadoux, Jannaud, van Wijngaarden, Luu, Wu

Abbreviations and Acronyms:
AMD = age-related macular degeneration; **CERA** = Centre for Eye Research Australia; **DACP** = dark-adapted chromatic perimeter; **NIR** = near-infrared reflectance; **PWSD** = pointwise sensitivity difference; **RIT** = rod intercept time; **RPD** = reticular pseudodrusen.

Keywords:
Age-related macular degeneration, Reticular pseudodrusen, Dark adaptation, Rod photoreceptors, Drusen.

Correspondence:
Zhichao Wu, Centre for Eye Research Australia, Royal Victorian Eye and Ear Hospital, Level 7, 32 Gisborne Street, East Melbourne, VIC 3002, Australia. E-mail: wu.z@unimelb.edu.au.

References

1. Wu Z, Fletcher EL, Kumar H, et al. Reticular pseudodrusen: A critical phenotype in age-related macular degeneration. *Prog Retin Eye Res*. 2022;88:101017.
2. Finger RP, Wu ZC, Luu CD, et al. Reticular pseudodrusen: a risk factor for geographic atrophy in fellow eyes of individuals with unilateral choroidal neovascularization. *Ophthalmology*. 2014;121:1252−1256.
3. Zhou Q, Shaffer J, Ying GS. Pseudodrusen in the fellow eye of patients with unilateral neovascular age-related macular degeneration: a meta-analysis. *PLoS One*. 2016;11:e0149030.
4. Nassisi M, Lei J, Abdelfattah NS, et al. OCT risk factors for development of late age-related macular degeneration in the fellow eyes of patients enrolled in the HARBOR study. *Ophthalmology*. 2019;126:1667−1674.
5. Agrón E, Domalpally A, Cukras CA, et al. Reticular pseudodrusen: the third macular risk feature for progression to late age-related macular degeneration: Age-Related Eye Disease Study 2 report 30. *Ophthalmology*. 2022;129:1107−1119.
6. Holmen IC, Aul B, Pak JW, et al. Precursors and Development of Geographic Atrophy with Autofluorescence Imaging: Age-Related Eye Disease Study 2 report number 18. *Ophthalmol Retina*. 2019;3:724−733.
7. Reiter GS, Told R, Schranz M, et al. Subretinal drusenoid deposits and photoreceptor loss detecting global and local progression of geographic atrophy by SD-OCT imaging. *Invest Ophthalmol Vis Sci*. 2020;61:11.
8. Guymer RH, Wu ZC, Hodgson LAB, et al. Subthreshold nanosecond laser intervention in age-related macular degeneration: the LEAD randomized controlled clinical trial. *Ophthalmology*. 2019;126:829−838.
9. Greferath U, Guymer RH, Vessey KA, et al. Correlation of histologic features with in vivo imaging of reticular pseudodrusen. *Ophthalmology*. 2016;123:1320−1331.
10. Chen L, Messinger JD, Zhang Y, et al. Subretinal drusenoid deposit in age-related macular degeneration: histologic insights into initiation, progression to atrophy, and imaging. *Retina*. 2020;40:618−631.
11. Mrejen S, Sato T, Curcio CA, Spaide RF. Assessing the cone photoreceptor mosaic in eyes with pseudodrusen and soft Drusen in vivo using adaptive optics imaging. *Ophthalmology*. 2014;121:545−551.
12. Zhang Y, Wang X, Sadda SR, et al. Lifecycles of individual subretinal drusenoid deposits and evolution of outer retinal atrophy in age-related macular degeneration. *Ophthalmol Retina*. 2020;4:274−283.
13. Tan RS, Guymer RH, Aung KZ, et al. Longitudinal assessment of rod function in intermediate age-related macular degeneration with and without reticular pseudodrusen. *Invest Ophthalmol Vis Sci*. 2019;60:1511−1518.
14. Fraser RG, Tan R, Ayton LN, et al. Assessment of retinotopic rod photoreceptor function using a dark-adapted chromatic perimeter in intermediate age-related macular degeneration. *Invest Ophthalmol Vis Sci*. 2016;57:5436−5442.
15. Laíns I, Miller JB, Park DH, et al. Structural changes associated with delayed dark adaptation in age-related macular degeneration. *Ophthalmology*. 2017;124:1340−1352.
16. Flamendorf J, Agrón E, Wong WT, et al. Impairments in dark adaptation are associated with age-related macular

degeneration severity and reticular pseudodrusen. *Ophthalmology*. 2015;122:2053−2062.
17. Sevilla MB, McGwin G Jr, Lad EM, et al. Relating retinal morphology and function in aging and early to intermediate age-related macular degeneration subjects. *Am J Ophthalmol*. 2016;165:65−77.
18. Flynn OJ, Cukras CA, Jeffrey BG. Characterization of rod function phenotypes across a range of age-related macular degeneration severities and subretinal drusenoid deposits. *Invest Ophthalmol Vis Sci*. 2018;59:2411−2421.
19. Pondorfer SG, Wintergerst MWM, Gorgi Zadeh S, et al. Association of visual function measures with drusen volume in early stages of age-related macular degeneration. *Invest Ophthalmol Vis Sci*. 2020;61:55.
20. Crossland MD, Tufail A, Rubin GS, Stockman A. Mesopic microperimetry measures mainly cones; dark-adapted microperimetry measures rods and cones. *Invest Ophthalmol Vis Sci*. 2012;53:4822.
21. Han RC, Gray JM, Han J, et al. Optimisation of dark adaptation time required for mesopic microperimetry. *Br J Ophthalmol*. 2019;103:1092−1098.
22. Simunovic MP, Moore AT, MacLaren RE. Selective automated perimetry under photopic, mesopic, and scotopic conditions: detection mechanisms and testing strategies. *Transl Vis Sci Technol*. 2016;5:10.
23. Kumar H, Guymer RH, Hodgson LAB, et al. Exploring reticular pseudodrusen extent and impact on mesopic visual sensitivity in intermediate age-related macular degeneration. *Invest Ophthalmol Vis Sci*. 2022;63:14.
24. Wu Z, Luu CD, Hodgson LAB, et al. Prospective longitudinal evaluation of nascent geographic atrophy in age-related macular degeneration. *Ophthalmol Retina*. 2020;4:568−575.
25. Thomas MM, Lamb TD. Light adaptation and dark adaptation of human rod photoreceptors measured from the a-wave of the electroretinogram. *J Physiol*. 1999;518:479−496.
26. Dimitrov PN, Guymer RH, Zele AJ, et al. Measuring rod and cone dynamics in age-related maculopathy. *Invest Ophthalmol Vis Sci*. 2008;49:55−65.
27. Gunawan JR, Thiele SH, Isselmann B, et al. Effect of subthreshold nanosecond laser on retinal structure and function in intermediate age-related macular degeneration. *Clin Exp Ophthalmol*. 2022;50:31−39.
28. Luu CD, Tan R, Caruso E, et al. Topographic rod recovery profiles after a prolonged dark adaptation in subjects with reticular pseudodrusen. *Ophthalmol Retina*. 2018;2:1206−1217.
29. Uddin D, Jeffrey BG, Flynn O, et al. Repeatability of scotopic sensitivity and dark adaptation using a Medmont dark-adapted chromatic perimeter in age-related macular degeneration. *Transl Vis Sci Technol*. 2020;9:31.
30. Tan R, Guymer RH, Luu CD. Subretinal drusenoid deposits and the loss of rod function in intermediate age-related macular degeneration. *Invest Ophthalmol Vis Sci*. 2018;59:4154−4161.
31. Goh KL, Abbott CJ, Hadoux X, et al. Hyporeflective cores within drusen: association with progression of age-related macular degeneration and impact on visual sensitivity. *Ophthalmol Retina*. 2022;6:284−290.
32. Gorgi Zadeh S, Wintergerst MWM, Wiens V, et al. CNNs enable accurate and fast segmentation of drusen in optical coherence tomography. In: Cardoso MJ, Arbel T, Carneiro G, et al., eds. *Deep Learning in Medical Image Analysis and Multimodal Learning for Clinical Decision Support*. Cham: Springer International Publishing; 2017: 65−73.
33. Querques G, Massamba N, Srour M, et al. Impact of reticular pseudodrusen on macular function. *Retina*. 2014;34: 321−329.
34. Ooto S, Suzuki M, Vongkulsiri S, et al. Multimodal visual function testing in eyes with nonexudative age-related macular degeneration. *Retina*. 2015;35:1726−1734.
35. Wu Z, Ayton LN, Makeyeva G, et al. Impact of reticular pseudodrusen on microperimetry and multifocal electroretinography in intermediate age-related macular degeneration. *Invest Ophthalmol Vis Sci*. 2015;56:2100−2106.
36. Steinberg JS, Saßmannshausen M, Fleckenstein M, et al. Correlation of partial outer retinal thickness with scotopic and mesopic fundus-controlled perimetry in patients with reticular drusen. *Am J Ophthalmol*. 2016;168:52−61.
37. Sassmannshausen M, Pfau M, Thiele S, et al. Longitudinal analysis of structural and functional changes in presence of reticular pseudodrusen associated with age-related macular degeneration. *Invest Ophthalmol Vis Sci*. 2020;61:19.
38. Chiang TTK, Keenan TD, Agrón E, et al. Macular thickness in intermediate age-related macular degeneration is influenced by disease severity and subretinal drusenoid deposit presence. *Invest Ophthalmol Vis Sci*. 2020;61:59.
39. Nittala MG, Hogg RE, Luo Y, et al. Changes in retinal layer thickness in the contralateral eye of patients with unilateral neovascular age-related macular degeneration. *Ophthalmol Retina*. 2019;3:112−121.
40. Ramon C, Cardona G, Biarnés M, et al. Longitudinal changes in outer nuclear layer thickness in soft drusen and reticular pseudodrusen. *Clin Exp Optom*. 2019;102:601−610.
41. Laíns I, Wang J, Providência J, et al. Choroidal changes associated with subretinal drusenoid deposits in age-related macular degeneration using swept-source optical coherence tomography. *Am J Ophthalmol*. 2017;180:55−63.
42. Yohannan J, Wang J, Brown J, et al. Evidence-based criteria for assessment of visual field reliability. *Ophthalmology*. 2017;124:1612−1620.
43. Wu Z, Schmitz-Valckenberg S, Blodi BA, et al. Reticular pseudodrusen: interreader agreement of evaluation on OCT imaging in age-related macular degeneration. *Ophthalmol Sci*. 2023;3:100325.